

## **Supplementary Information**

### **Monocyte Preprogramming by Tobacco Carcinogens and Fructose Intake Accelerates Lung Cancer Progression via Metabolic and Epigenetic Pathways**

**Table S1. Primer sequences used for real-time PCR.**

<b>Species</b>	<b>Gene</b>	<b>Forward sequence (5'-3')</b>	<b>Reverse sequence (5'-3')</b>
Human	<i>CD1A</i>	ATACGCACCATTTCGGTCATTT	GCTCACAAAGTCTGATCCTTGAT
Human	<i>CD14</i>	ACGCCAGAACCTTGTGAGC	GCATGGATCTCCACCTCTACTG
Human	<i>CD68</i>	CTTCTCTCATTCCCCTATGGACA	GAAGGACACATTGTACTCCACC
Human	<i>ARG1</i>	TGGACAGACTAGGAATTGGCA	CCAGTCCGTCAACATCAAACT
Human	<i>CCL22</i>	CCCTACGGCGCCAACAT	CAGACGGTAACGGACGTAATCA
Human	<i>IL10</i>	GAACCAAGACCCAGACATC	CATTCTTCACCTGCTCCAC
Human	<i>TGFB1</i>	GACACCAACTATTGCTTCAG	CAGGCTCCAAATGTAGGG
Human	<i>VEGFA</i>	TTGCCTTGCTGCTCTACCTCCA	GATGGCAGTAGCTGCGCTGATA
Human	<i>MAFB</i>	TCAAGTTCGACGTGAAGAAGG	GTTTCATCTGCTGGTAGTTGCT
Human	<i>MAF</i>	GAGACCGACCGCATCATCAG	GGTAGCCGGTCATCCAGTAG
Human	<i>EGR1</i>	GGTCAGTGGCCTAGTGAGC	GTGCCGCTGAGTAAATGGGA
Human	<i>IL1B</i>	TGATGGCTTATTACAGTGGCAATG	GTAGTGGTGGTGGGAGATTCCG
Human	<i>NOS2</i>	GCTCTACACCTCCAATGTGACC	CTGCCGAGATTTGAGCCTCATG
Human	<i>SLC2A5</i>	ACGTTGCTGTGGTCTGTAACC	CATTAAGATCGCAGGCACGATA
Human	<i>SLC2A6</i>	CCGGACTACGACACCTTCC	GGATGTGTAGACCAGGGCATA
Human	<i>SLC2A7</i>	CAGTACGGCTACAACCTCTCT	TTGCGTGTGCTCAAAGTAGG
Human	<i>SLC2A8</i>	CTAGTGGCCCCGGTCTACAT	CCGACGACGACCATTAGCTG
Human	<i>SLC2A9</i>	CAATAGACCCAGACACTCTGACT	TCTTCACAATTAACGTCCCCAC
Human	<i>SLC2A10</i>	CTTGCTGTATCTACGTGTCAGA	CCAGCCAGTGCATAGTTGAGG
Human	<i>SLC2A11</i>	GGAGTCAATGCAGGTGTGAG	CCAGAGCCGTAAAGATGGCTG
Human	<i>SLC2A12</i>	GAGGCTGCGGCATGTTTAC	CCAAGTTCATAACCCACCAGG
Human	<i>SLC2A13</i>	ACATTGCGGAGGTCTCACC	AGGCTCCATCAACAACACTTG
Human	<i>SLC2A14</i>	CTGCTCACGAATCTCTGGTCC	GCCTAATAGCACCGGCCATAG
Human	<i>ACTB</i>	TCATTCCAAATATGAGATGCGTTG	TAGAGAGAAGTGGGGTGGCT

---

Mouse	<i>Sox2</i>	GCGGAGTGGAACTTTTGTCC	CGGGAAGCGTGTACTTATCCTT
Mouse	<i>Aldh1a1</i>	ATACTTGTCGGATTTAGGAGGCT	GGGCCTATCTTCCAAATGAACA
Mouse	<i>Ccl2</i>	TTAAAAACCTGGATCGGAACCAA	GCATTAGCTTCAGATTTACGGGT
Mouse	<i>Ccl7</i>	CAGAAGGATCACCAGTAGTCGG	ATAGCCTCCTCGACCCACTTCT
Mouse	<i>Slc2a7</i>	GATTCTCCTGCTGTCTGGCTAT	GATGGATGGAAACGTCAACC
Mouse	<i>Slc2a8</i>	TTCATGGCCTTTCTAGTGACC	GAGTCCTGCCTTTAGTCTCAG
Mouse	<i>Slc2a9</i>	TGCTTCCTCGTCTTCGCCACAATA	CTCTTGGCAAATGCCTGGCTGATT
Mouse	<i>Gapdh</i>	GAGTTGCTGTTGAAGTCGCA	GGTGGTGAAGCAGGCATCTG

---

**Table S2. Primer sequences used for chromatin immunoprecipitation assay\***

Name	Forward sequence (5'-3')	Reverse sequence (5'-3')
ARG1_H3K9ac	GATTCTACAATTATTTTCCTG	CATGAGGGTAAATGGTTAATC
ARG1_STAT3	GAAATGTGTCTCATGGATTAAC	CGTCCTTGTAGAAGAAGGGCC
IL10_STAT3/H3 K9ac	GGAGGAGCTCTAAGCAGAA	AAGCCCCTGATGTGTAGAC
VEGFA_STAT3/ H3K9ac	CTTCCCGTTCTCAGCTCCACAAAC	CTGGCCTGCAGACATCAAAGTGAG

\*We conducted a chromatin immunoprecipitation assay for evaluating the binding of acetylated H3 at the lysine 9 residue (H3K9ac) or STAT3 to the *MAFB*, *MAF*, or *EGR1* promoters by using primers available in the previous report (DOI: <https://doi.org/10.1016/j.molcel.2020.05.004>).

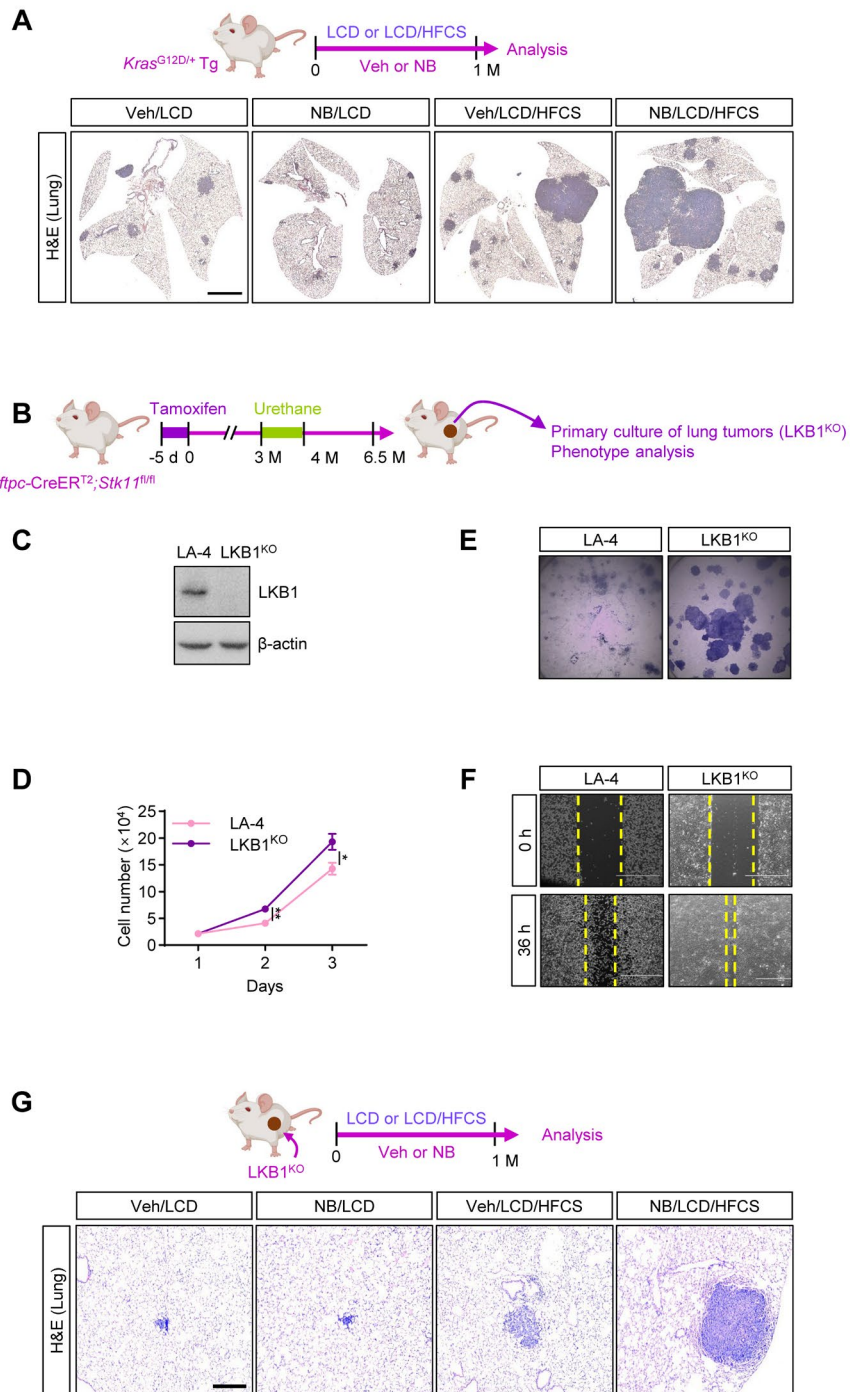
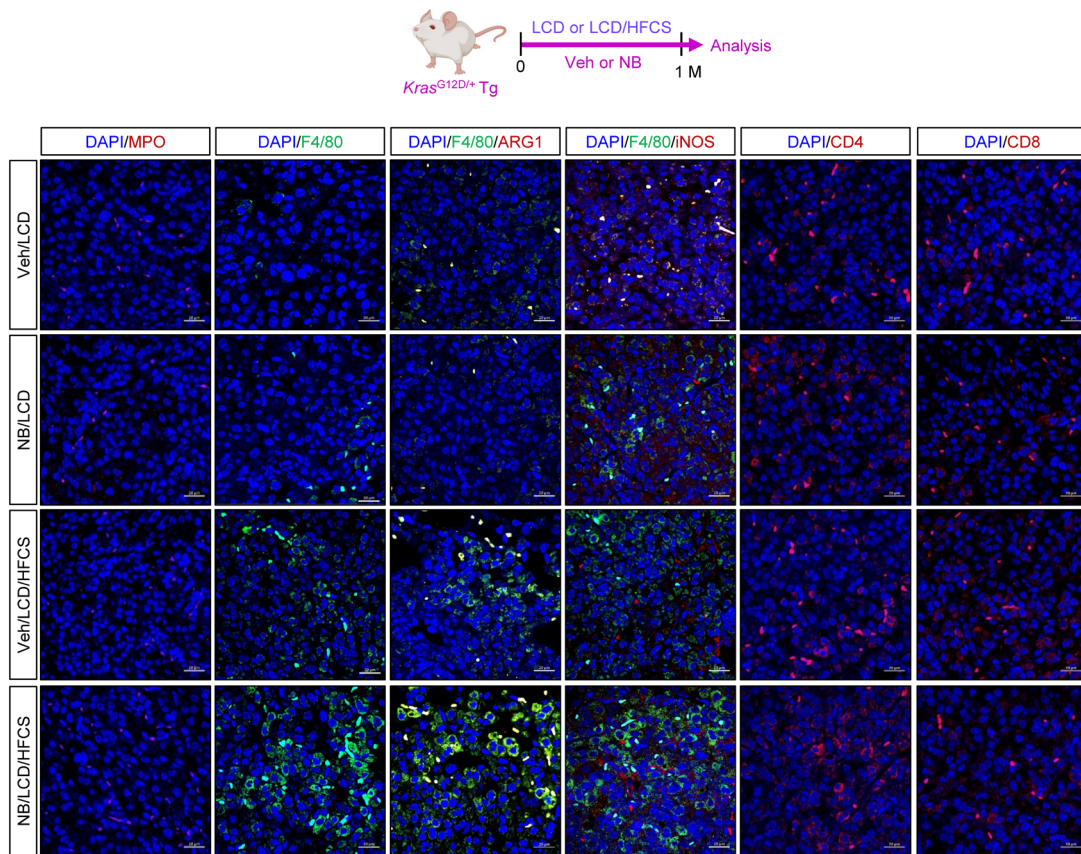


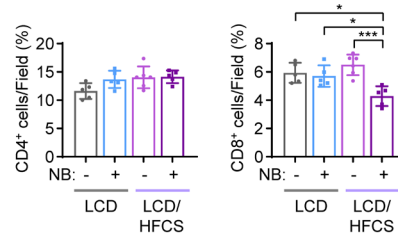
**Figure S1. High-fructose corn syrup (HFCS) accelerates the 4-(methylnitrosamino)-1-(3-pyridyl)-1-butanol- and benzo[a]pyrene (NB)-induced lung tumorigenesis and characterization of LKB1<sup>KO</sup> cells. (A)** Representative images of H&E-stained lung tissues from *Kras*<sup>G12D/+</sup> Tg mice treated with either vehicle (Veh) or NB and fed a low-carbohydrate diet (LCD) or an LCD supplemented with high fructose corn syrup (HFCS, LCD/HFCS). Scale bar, 3 mm. **(B)** Schematic diagram illustrating the experimental protocol to establish LKB1<sup>KO</sup> primary lung cancer cells. **(C)** Representative western blot analysis images for evaluating the level of LKB1 expression in LKB1<sup>KO</sup> cells in comparison with LA-4 cells. **(D)** Changes in cell proliferation of LA-4 and LKB1<sup>KO</sup>

cells, as determined by cell counting assay (mean  $\pm$  SD,  $n = 3$ ). \* $p < 0.05$  and \*\* $p < 0.01$ , as determined by a two-tailed Student's  $t$ -test. (E) Representative images showing changes in anchorage-dependent colony formation in LKB1<sup>KO</sup> cells in comparison with LA-4 cells, as determined by anchorage-dependent colony formation assay. (F) Representative images showing changes in the migratory ability of LKB1<sup>KO</sup> cells compared to LA-4 cells, as determined by a scratch assay. Scale bars, 1000  $\mu\text{m}$ . (G) Representative images of H&E-stained lung tissues of the indicated groups. Scale bar, 200  $\mu\text{m}$ .

**A**



**B**



**C**

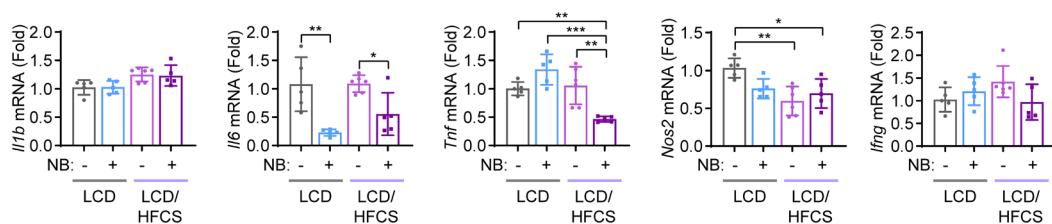


**Figure S2. Fructose supplementation promotes monocyte differentiation and M2 polarization in the *Kras*<sup>G12D/+</sup> transgenic (Tg) mouse model.** (A) Schematic diagram illustrating the experimental timeline and representative immunofluorescence images showing infiltration of MPO<sup>+</sup> neutrophils, F4/80<sup>+</sup> macrophages, M1 macrophages (F4/80<sup>+</sup>iNOS<sup>+</sup>), M2 macrophages (F4/80<sup>+</sup>ARG1<sup>+</sup>), CD4<sup>+</sup> T cells, and CD8<sup>+</sup> T cells in lung tumors from *Kras*<sup>G12D/+</sup> Tg mice treated with vehicle (Veh) or NB and fed a low-carbohydrate diet (LCD) or an LCD supplemented with high fructose corn syrup (HFCS, LCD/HFCS). Quantification of MPO<sup>+</sup>, F4/80<sup>+</sup>, F4/80<sup>+</sup>iNOS<sup>+</sup>, and F4/80<sup>+</sup>ARG1<sup>+</sup> cells is presented in **Fig. 2E**. Scale bars, 20  $\mu$ m. (B) Quantification of CD4<sup>+</sup> and CD8<sup>+</sup>

T cells (mean  $\pm$  SD,  $n = 5$  or  $6$ ). **(C)** Real-time PCR analysis of the indicated genes in lung tumors derived from the specified groups of *Kras*<sup>G12D/+</sup> Tg mice (mean  $\pm$  SD,  $n = 5$  or  $6$ ). \* $p < 0.05$ , \*\* $p < 0.01$ , and \*\*\* $p < 0.001$ , as determined by one-way ANOVA with Dunnett's multiple-comparison test **(B, C)**.

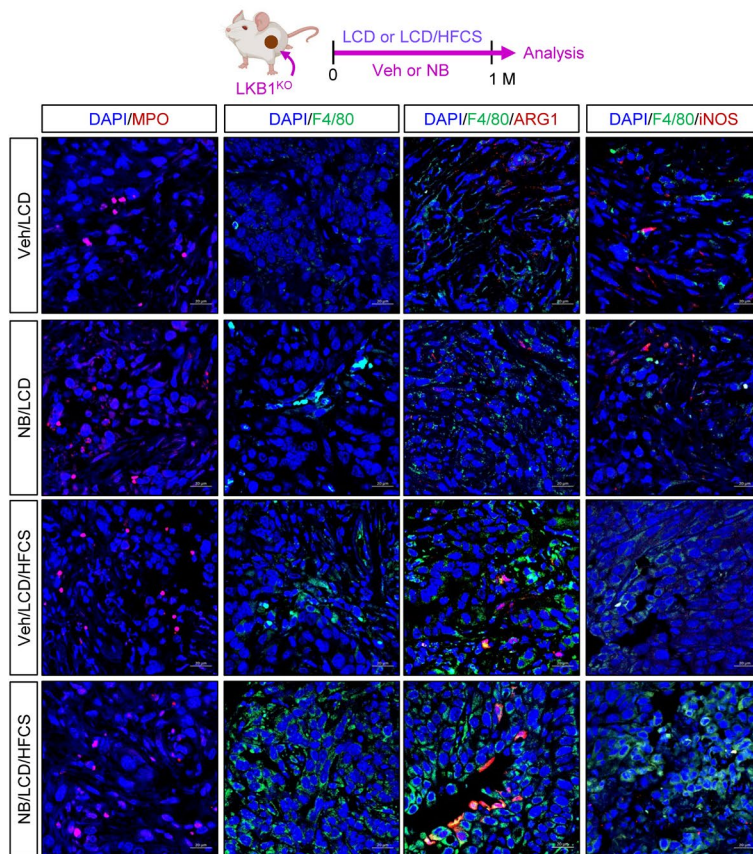


**Figure S3. Fructose supplementation promotes the differentiation and polarization of monocytes into M2 macrophages in the LKB1<sup>KO</sup> allograft model.** Schematic diagram illustrating the experimental timeline and representative immunofluorescence images showing the infiltration of MPO<sup>+</sup> neutrophils, F4/80<sup>+</sup> macrophages, M1 macrophages (F4/80<sup>+</sup>iNOS<sup>+</sup>), and M2 macrophages (F4/80<sup>+</sup>ARG1<sup>+</sup>) in subcutaneous LKB1<sup>KO</sup> tumors from mice treated with vehicle (Veh) or NB under the conditions of LCD or LCD/HFCS. Quantitative analysis results are presented in **Fig. 2I**. Scale bars, 20  $\mu$ m.

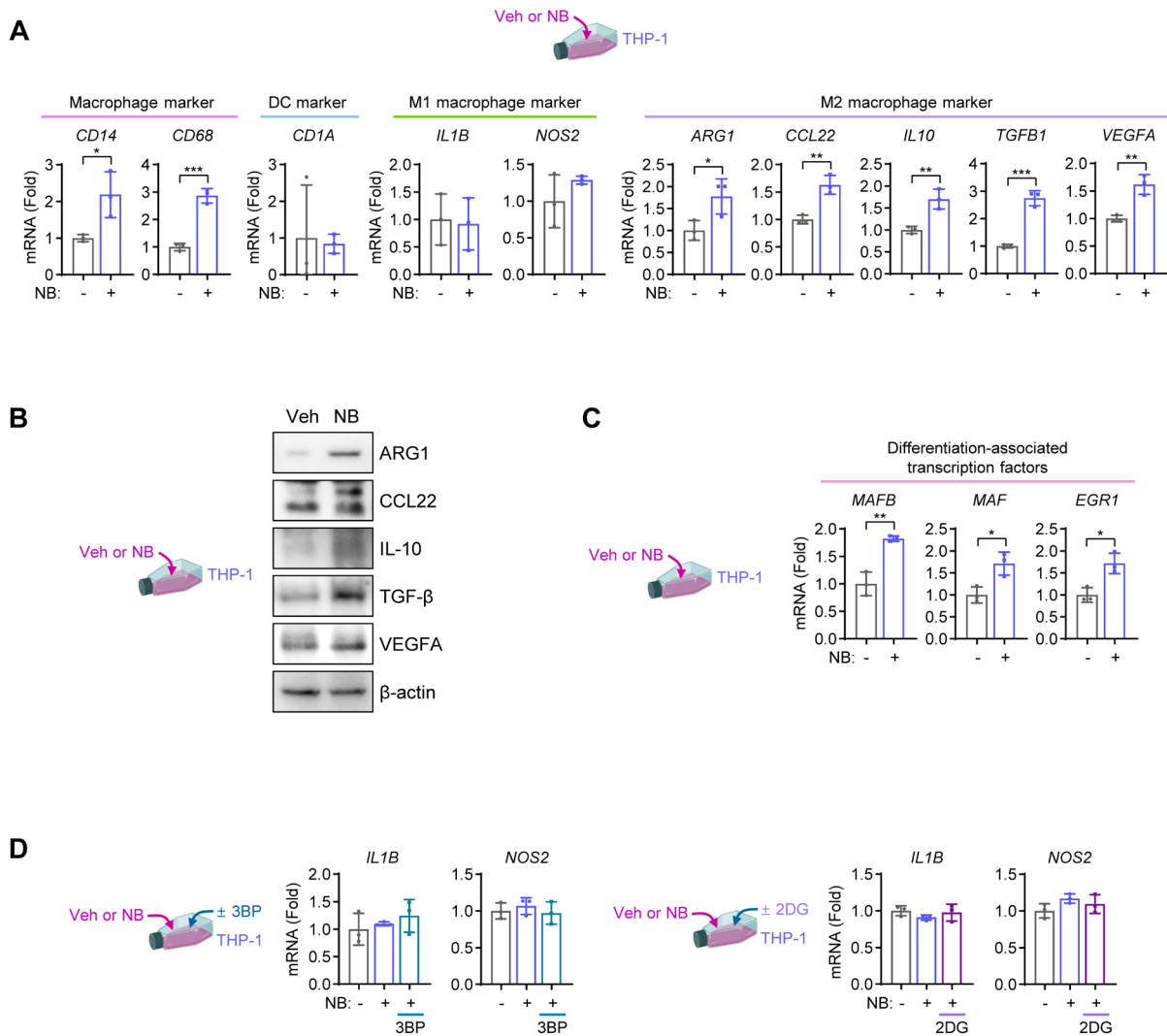


**Figure S4. 4-(methylnitrosamino)-1-(3-pyridyl)-1-butanol- and benzo[a]pyrene (NB) induces the expression of M2 macrophage-associated markers.** THP-1 cells were treated with NB for three days under standard culture conditions, either alone or in combination with 3-bromopyruvate (3BP, 25  $\mu$ M) or 2-deoxy-D-glucose (2DG, 5 mM). **(A)** Real-time PCR analysis of mRNA expression levels of macrophage markers, dendritic cell (DC) markers, and M1- and M2-associated genes in THP-1 cells with or without NB treatment (mean  $\pm$  SD,  $n = 3$ ). **(B)** Western blot analysis of ARG1, CCL22, IL-10, TGF- $\beta$ , and VEGFA expression in THP-1 cells with or without NB treatment. **(C)** Real-time PCR analysis of differentiation-associated transcription factors (*MAFB*, *MAF*, and *EGR1*) in THP-1 cells with or without NB treatment (mean  $\pm$  SD,  $n = 3$ ). **(D)** Real-time PCR analysis of the indicated genes in THP-1 cells treated with NB, either alone or in combination with 3BP or 2DG (mean  $\pm$  SD,  $n = 3$ ). \* $p < 0.05$ , \*\* $p < 0.01$ , and \*\*\* $p < 0.001$ , as determined by a two-tailed Student's  $t$ -test **(A, C)**. The differences among groups were not significant, as determined by one-way ANOVA with Tukey's multiple-comparison test **(D)**.